Molecular Cell, Volume *53*
Supplemental Information

Polycomb-Dependent H3K27me1 and H3K27me2 Regulate Active Transcription and Enhancer Fidelity

Karin J. Ferrari, Andrea Scelfo, SriGanesh Jammula, Alessandro Cuomo, Iros Barozzi, Alexandra Stützer, Wolfgang Fischle, Tiziana Bonaldi, and Diego Pasini

Ferrari et al. Figure S1

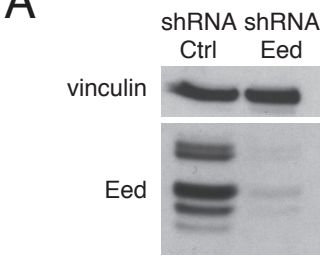

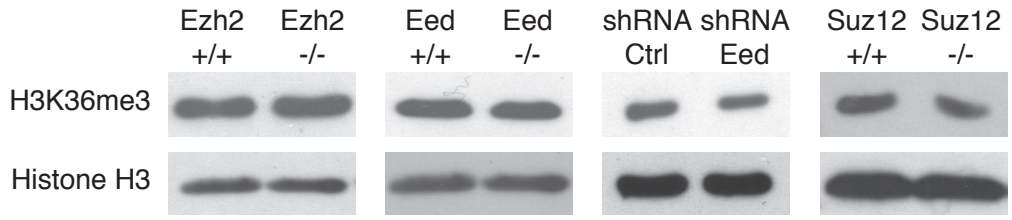

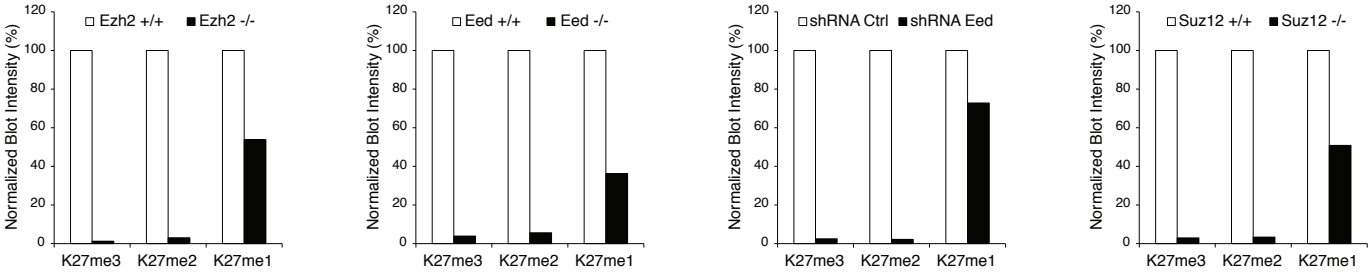

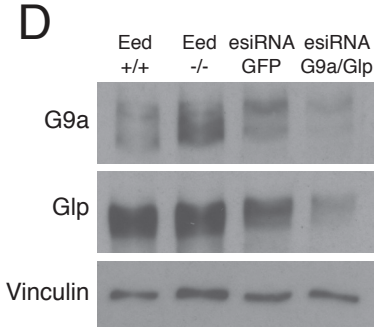

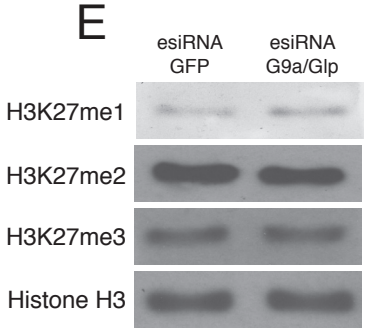

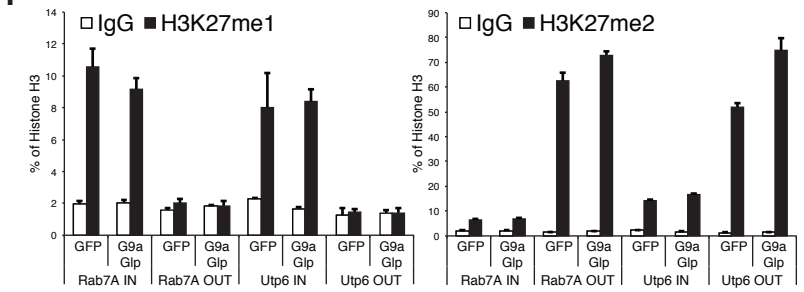

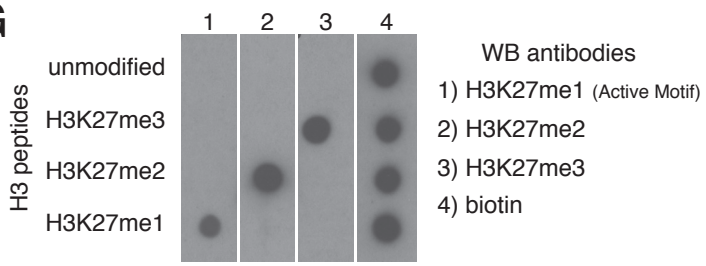

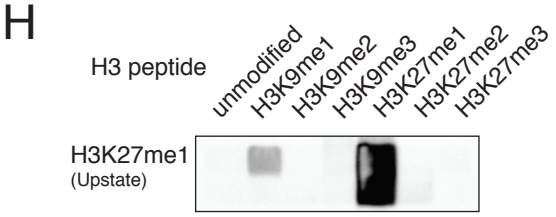

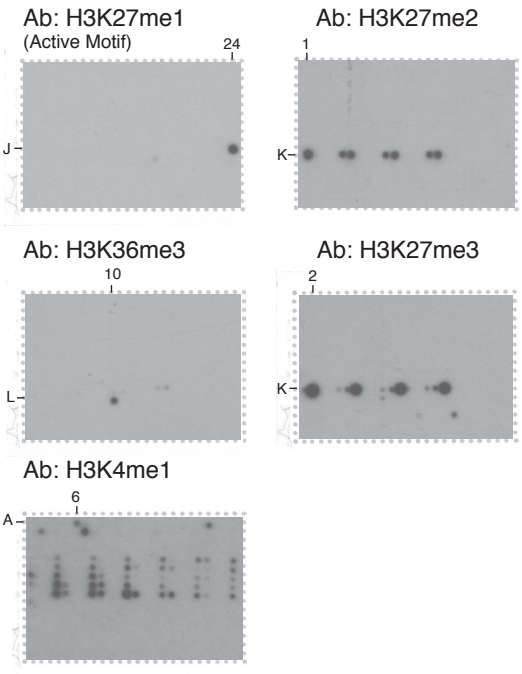

J

Antibodies specificity

Modified Peptides	Ab: H3K27me1	Ab: H3K27me2	Ab: H3K27me3	Ab: H3K36me3	Ab: H3K4me1
H3K27me1 (J24)	+++	-	-	-	-
H3K27me2 (K1)	-	+++	+	-	-
H3K27me3 (K2)	-	-	+++	-	-
H3K36me1 (L8)	-	-	-	-	-
H3K36me2 (L9)	-	-	-	-	-
H3K36me3 (L10)	-	-	-	+++	-
H3K4me1 (A6)	-	-	-	-	+++
H3K4me2 (A7)	-	-	-	-	+/-
H3K4me3 (A8)	-	-	-	-	-
H3K9me1 (A13)	-	-	-	-	-
H3K9me2 (A14)	-	-	-	-	-
H3K9me3 (A15)	-	-	-	-	-

Antibodies cross-reactivity

Modified Peptides	Ab: H3K27me1	Ab: H3K27me2	Ab: H3K27me3	Ab: H3K36me3	Ab: H3K4me1
	---	H3R26me2sK27me1 (K5): + H3R26me2aK27me1 (K10): + H3R26CitrK27me1 (K15): +	H3R26me2sK27me1 (K5): + H3R26me2sK27me2 (K6): + H3R26me2aK27me1 (K10): + H3R26me2aK27me2 (K11): + H3R26CitrK27me1 (K15): + H3R26CitrK27me2 (K16): +	---	H3R2me2sK4me2K9me3 (E21): +/- H3R2me2aK4me2K9ac (F1): + H3K4me2R8me2aK9me3 (G1): + H3K4me2R8me2aK9ac (G9): +/- H3R2me2sK4me2R8me2sK9me2 (G21): +/- H3R2me2aK4me2R8me2sK9me2 (H1): +/- H3R2me2sK4me2R8me2sK9me3 (H5): +/- H3R2me2aK4me2R8me2sK9me3 (H9): + H3R2me2sK4me2R8me2aK9me1 (H21): +/- H3R2me2sK4me2R8me2aK9me2 (I5): + H3R2me2aK4me2R8me2aK9me2 (I9): + H3R2me2sK4me2R8me2aK9me3 (I13): +/- H3R2me2aK4me2R8me2aK9me3 (I17): +/- H3R2me2sK4me2R8me2aK9ac (I21): +/-

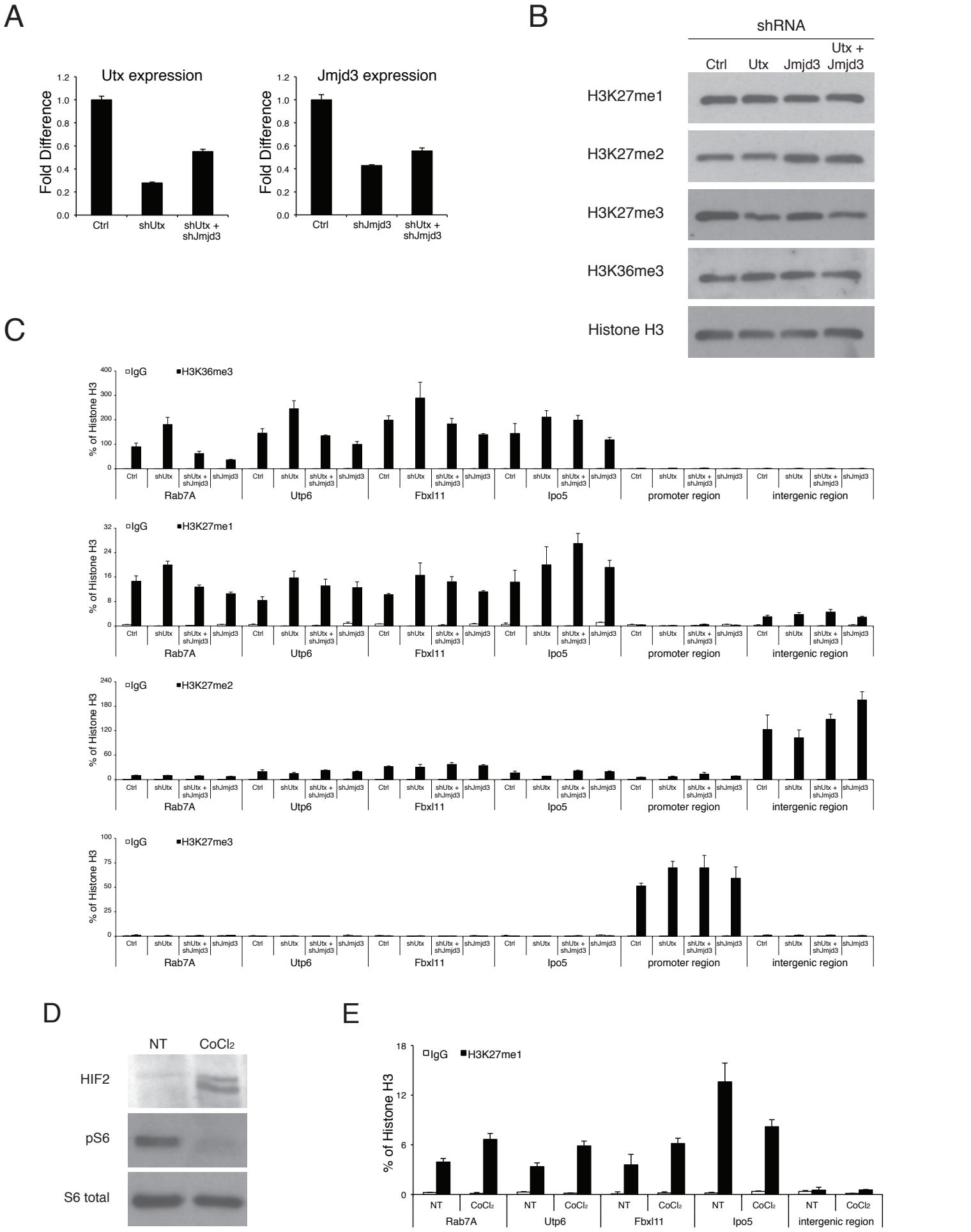
A
Utx expression
Fold Difference
Ctrl
shUtx
shUtx + shJmjd3
Jmjd3 expression
shJmjd3
B
shRNA
Ctrl
Utx
Jmjd3
Utx + Jmjd3
H3K27me1
H3K27me2
H3K27me3
H3K36me3
Histone H3
C
IgG
H3K36me3
H3K27me1
H3K27me2
H3K27me3
% of Histone H3
Rab7A
Utp6
Fbxl11
Ipo5
promoter region
intergenic region
D
NT
CoCl2
HIF2
pS6
S6 total
E
IgG
H3K27me1
% of Histone H3
NT
CoCl2
Rab7A
Utp6
Fbxl11
Ipo5
intergenic region

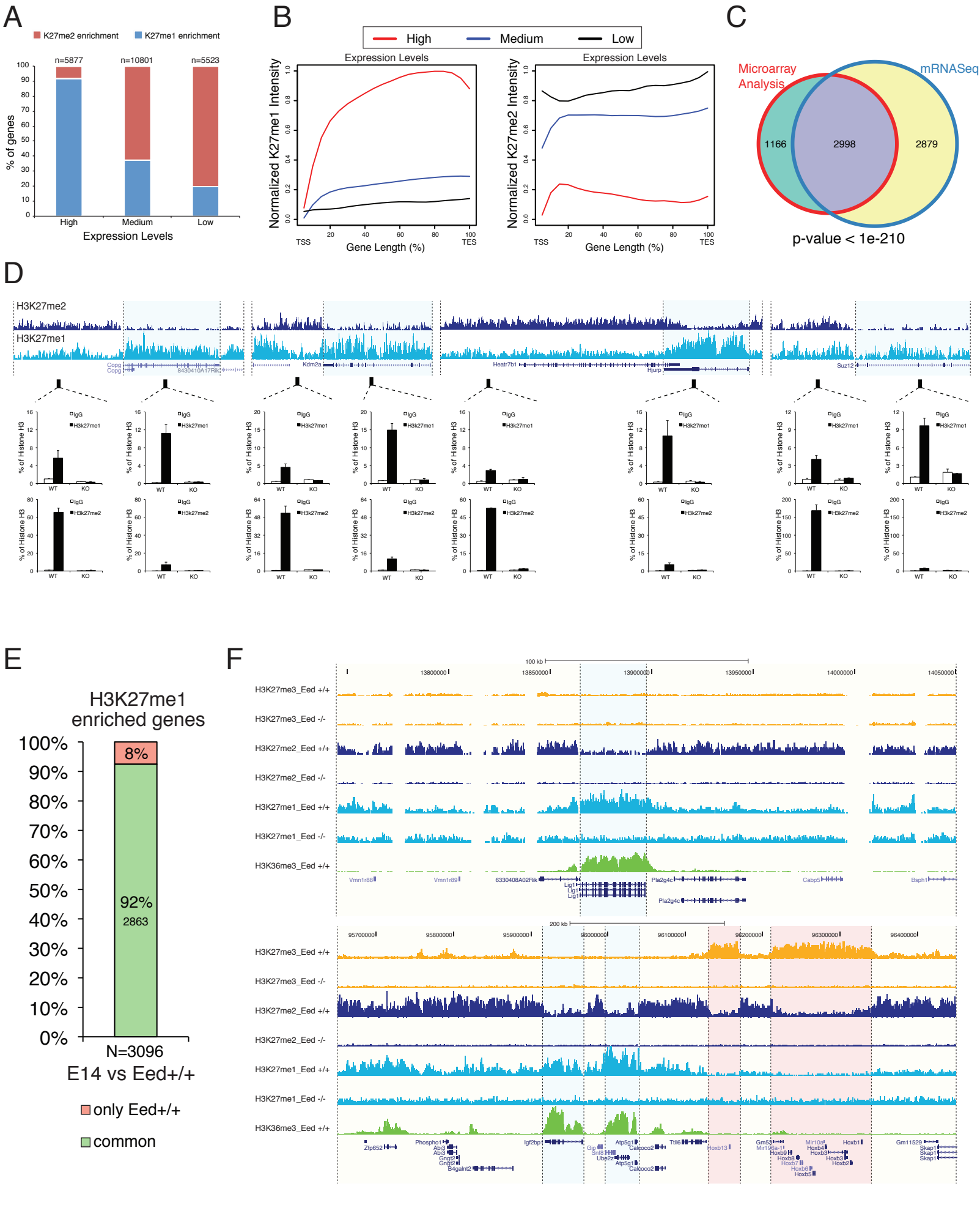
A
K27me2 enrichment
K27me1 enrichment
n=5877
n=10801
n=5523
% of genes
High
Medium
Low
Expression Levels
B
High
Medium
Low
Expression Levels
Normalized K27me1 Intensity
TSS
Gene Length (%)
TES
Expression Levels
Normalized K27me2 Intensity
TSS
Gene Length (%)
TES
C
Microarray Analysis
mRNASeq
1166
2998
2879
p-value < 1e-210
D
H3K27me2
H3K27me1
Copg
Copg
9430410A17Rik
Kdm2a
Heatr7b1
Hjurp
Suz12
IgG
H3K27me1
H3K27me2
% of Histone H3
WT
KO
E
H3K27me1
enriched genes
8%
92%
2863
N=3096
E14 vs Eed+/+
only Eed+/+
common
F
100 kb
13800000
13850000
13900000
13950000
14000000
14050000
H3K27me3_Eed +/+
H3K27me3_Eed -/-
H3K27me2_Eed +/+
H3K27me2_Eed -/-
H3K27me1_Eed +/+
H3K27me1_Eed -/-
H3K36me3_Eed +/+
Vmn1r88
Vmn1r89
6330408A02Rik
Lig1
Pla2g4c
Cabp5
Bsph1
200 kb
95700000
95800000
95900000
96000000
96100000
96200000
96300000
96400000
Zfp652
Phospho1
Abi3
Abi3
Gngt2
Gngt2
B4galnt2
Igf2bp1
Gip
Snf8
Ubp2z
Atp5g1
Atp5g1
Calcoco2
Calcoco2
Ttl6
Hoxb13
Gm53
Mir196a-1
Mir10al
Hoxb9
Hoxb8
Hoxb7
Hoxb6
Hoxb5
Hoxb4
Hoxb3
Hoxb2
Hoxb1
Gm11529
Skap1
Skap1
Skap1

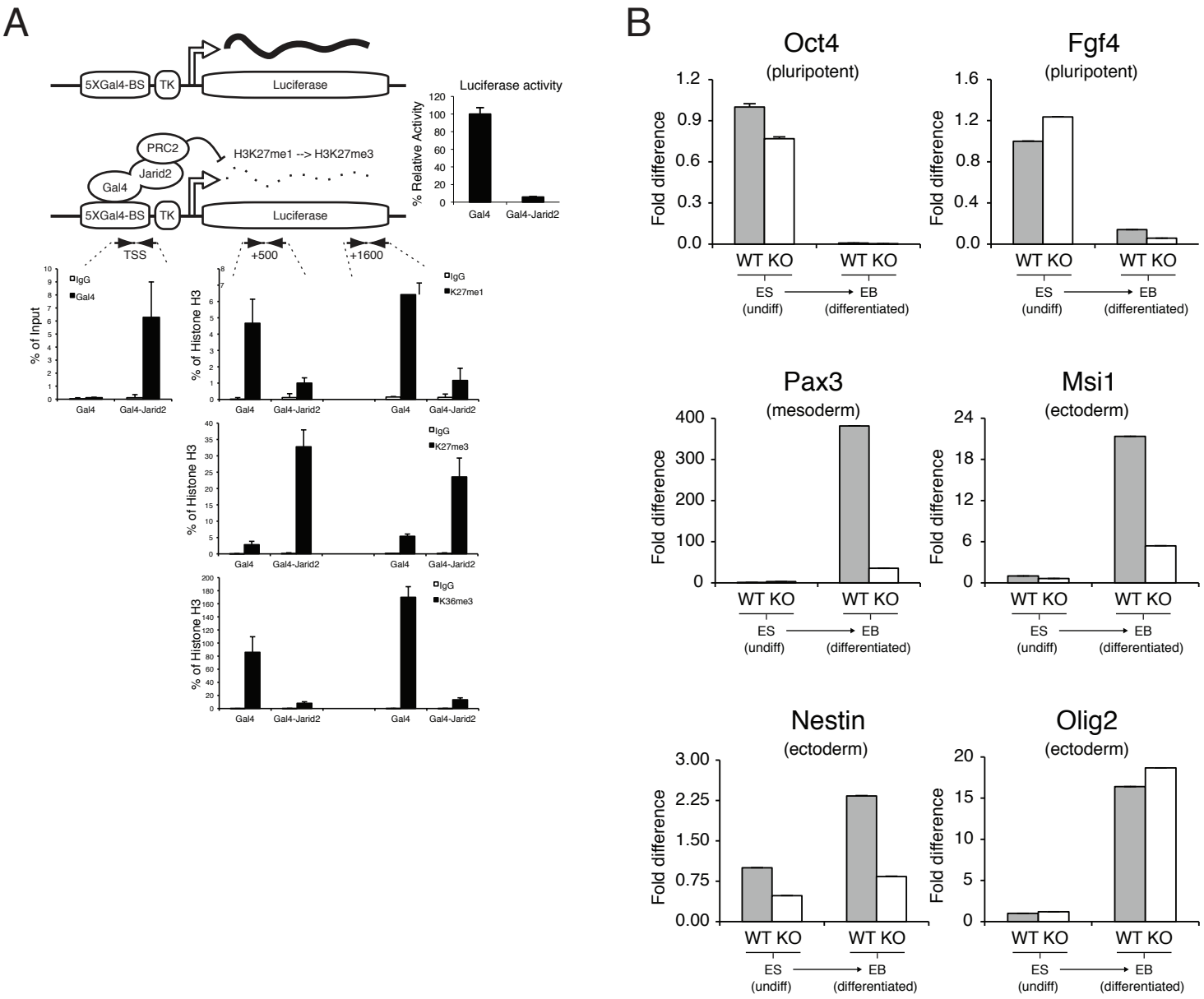
A
5XGal4-BS
TK
Luciferase
Luciferase activity
% Relative Activity
Gal4
Gal4-Jarid2
PRC2
Jarid2
H3K27me1 --> H3K27me3
TSS
+500
+1600
% of Input
% of Histone H3
IgG
K27me1
K27me3
K36me3
B
Oct4
(pluripotent)
Fgf4
(pluripotent)
Pax3
(mesoderm)
Msi1
(ectoderm)
Nestin
(ectoderm)
Olig2
(ectoderm)
Fold difference
WT KO
WT KO
ES
(undiff)
EB
(differentiated)
C
activation fold difference > 1.5
(n=394)
H3K27me1
EB Eed WT
EB Eed KO
Normalized Intensity
Gene Length(%)
p-Value=2.62e-66
FPKM
Expression Levels
WT
KO
WT
KO
ES
(undiff)
EB
(differentiated)

A

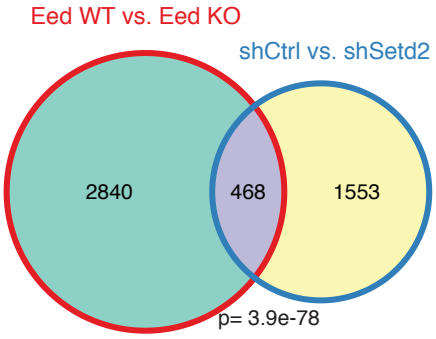

B

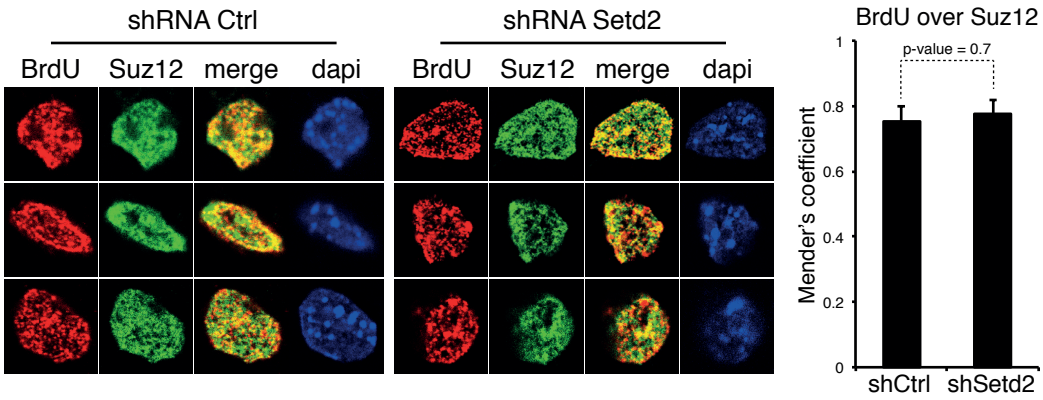

C

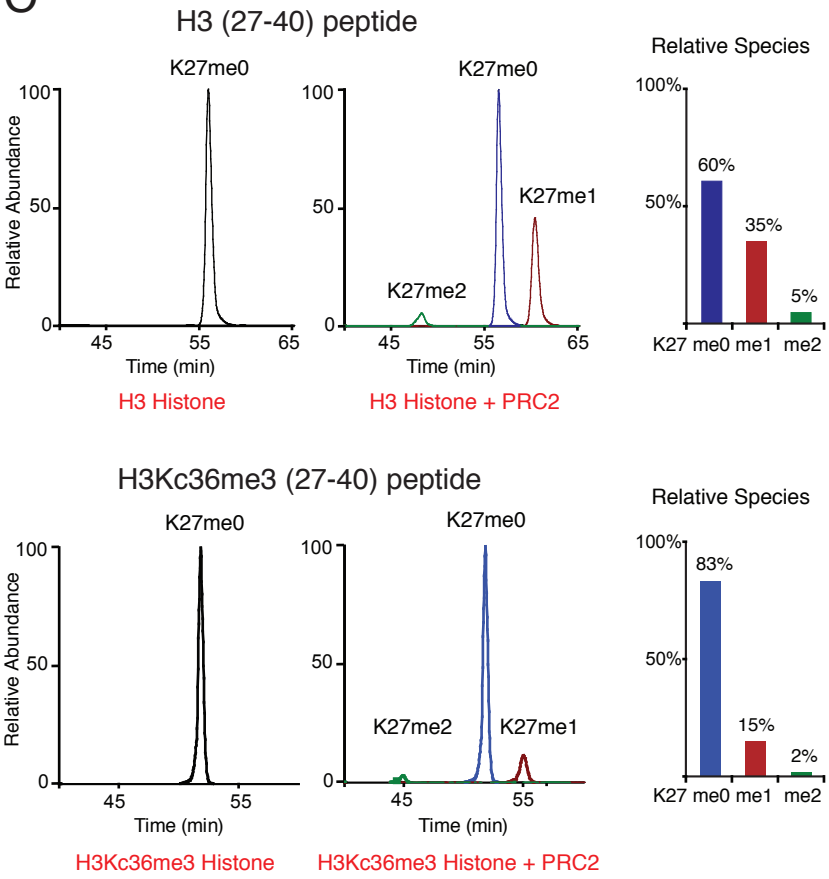

D

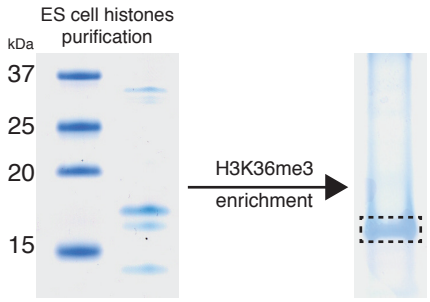

E

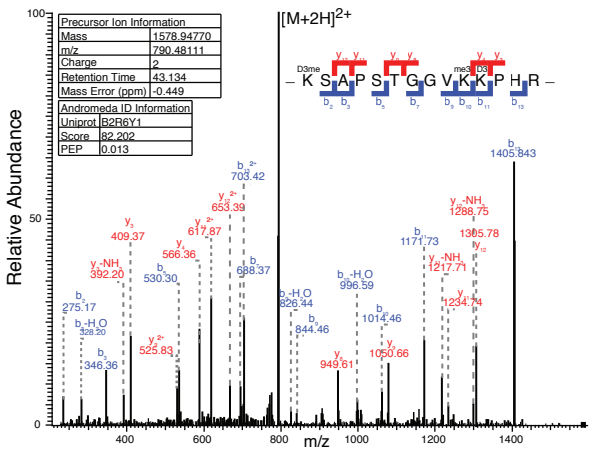

F

b ion-H₂O	b²⁺ ion	b ion				y ion	y²⁺ ion	y ion-NH₃
	mass	mass		seq		mass	mass	
--	--	188.1473	1	K(D3me)	14	--	--	--
--	--	275.1793	2	S	13	1392.815	--	--
328.2059	--	346.2164	3	A	12	1305.783	653.3951	1288.756
--	--	443.2692	4	P	11	1234.746	617.8765	1217.719
--	--	530.3012	5	S	10	1137.693	--	--
--	--	631.3489	6	T	9	1050.661	525.8341	--
--	--	688.3704	7	G	8	949.6133	--	--
--	--	745.3918	8	G	7	892.5919	--	--
826.4497	--	844.4602	9	V	6	835.5704	--	--
996.5916	--	1014.602	10	K(me3)	5	736.502	--	--
--	--	1171.732	11	K(D3)	4	566.3601	--	--
--	--	1268.784	12	P	3	409.2306	--	392.2041
--	703.4253	1405.843	13	H	2	312.1779	--	--
--	--	--	14	R	1	175.119	--	--

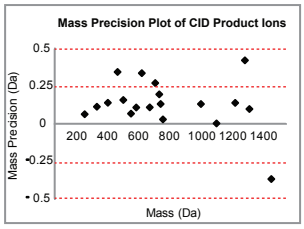

Annotation	
Protein	B2R6Y1
Protein Localisation	27-40
AminoAcid Coverage	79%
Method	ITMS, CID

Andromeda Search Configuration			
Variable Modification			
Title	Description	Specificity	ΔM (Da)
Lysines D3-acetylation (D3)	deuterate acetylation	K	45.0294
Lysines monomethylation (D3me)	D3-acetylation+monomethylation	K	59.0454
Lysines dimethylation (me2)	dimethylation	K	28.0310
Lysines trimethylation (me3)	trimethylation	K	42.0460

A

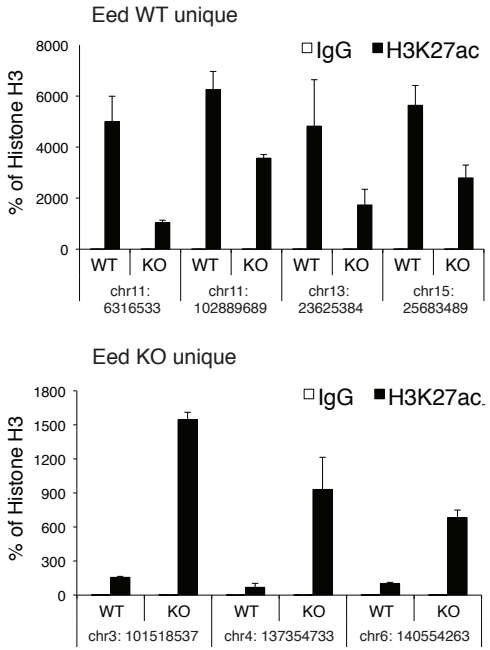
Eed WT unique
IgG
H3K27ac
% of Histone H3
8000
6000
4000
2000
0
WT
KO
chr11: 6316533
chr11: 102889689
chr13: 23625384
chr15: 25683489
Eed KO unique
IgG
H3K27ac
% of Histone H3
1800
1500
1200
900
600
300
0
chr3: 101518537
chr4: 137354733
chr6: 140554263

B

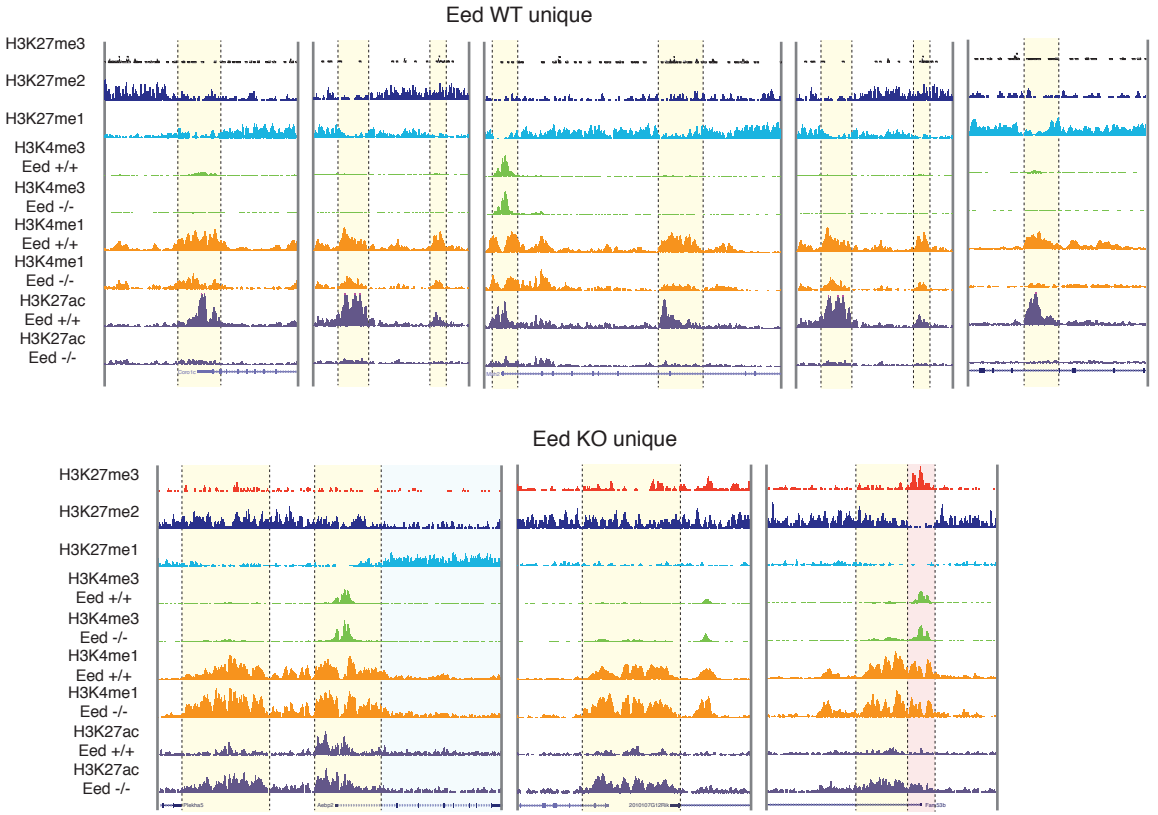
Eed WT unique
H3K27me3
H3K27me2
H3K27me1
H3K4me3 Eed +/+
H3K4me3 Eed -/-
H3K4me1 Eed +/+
H3K4me1 Eed -/-
H3K27ac Eed +/+
H3K27ac Eed -/-
Eed KO unique

C

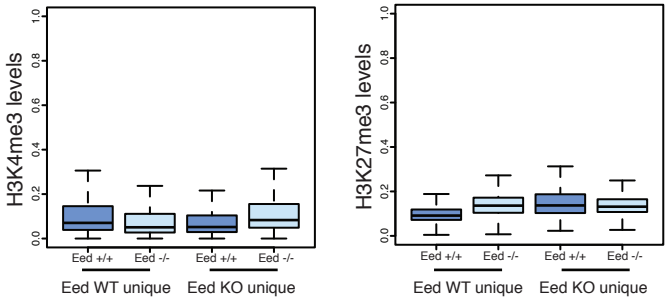
H3K4me3 levels
H3K27me3 levels
Eed +/+
Eed -/-
Eed WT unique
Eed KO unique

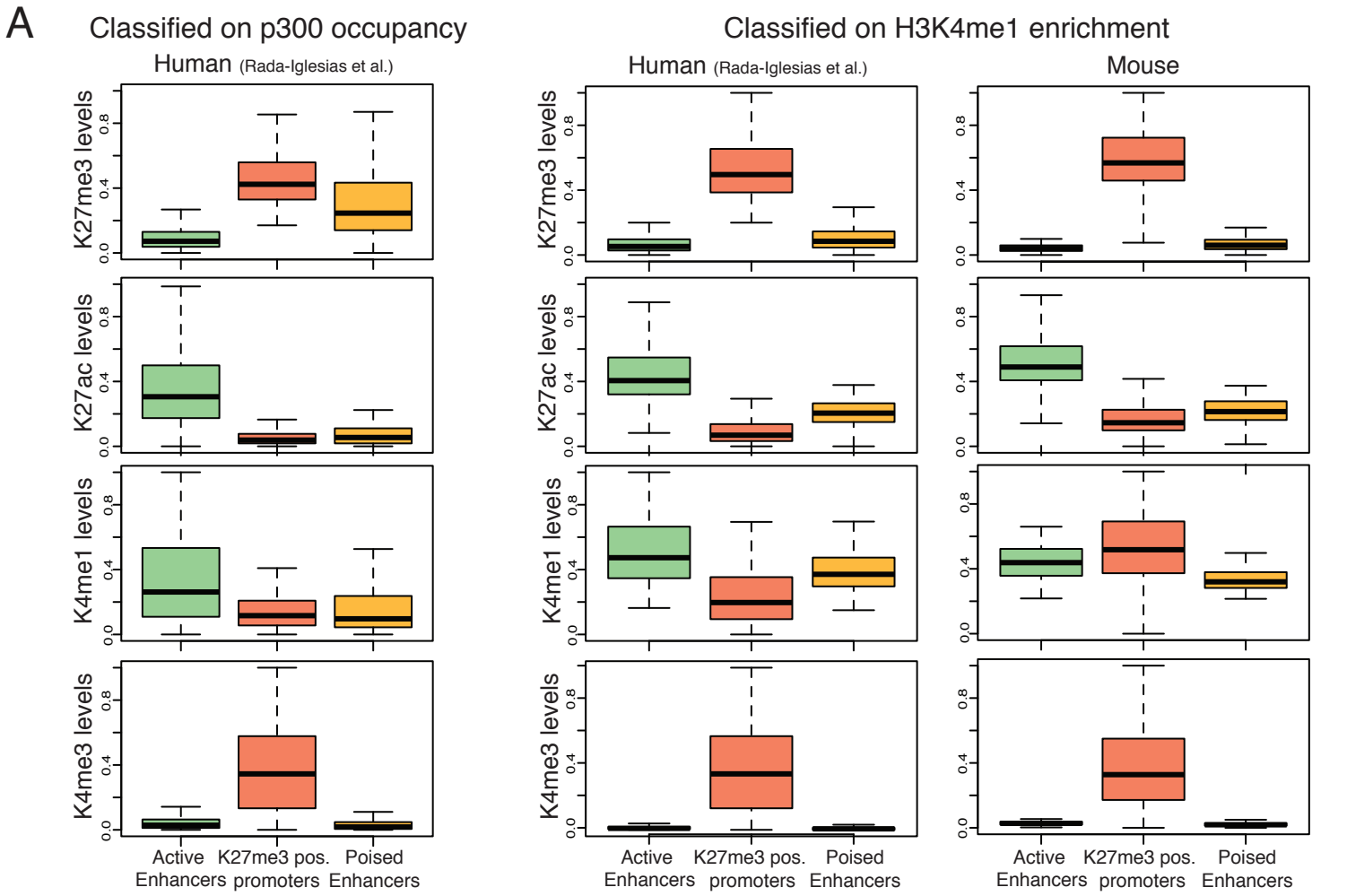
A
Classified on p300 occupancy
Human (Rada-Iglesias et al.)
Classified on H3K4me1 enrichment
Human (Rada-Iglesias et al.)
Mouse
K27me3 levels
K27ac levels
K4me1 levels
K4me3 levels
Active Enhancers
K27me3 pos. promoters
Poised Enhancers

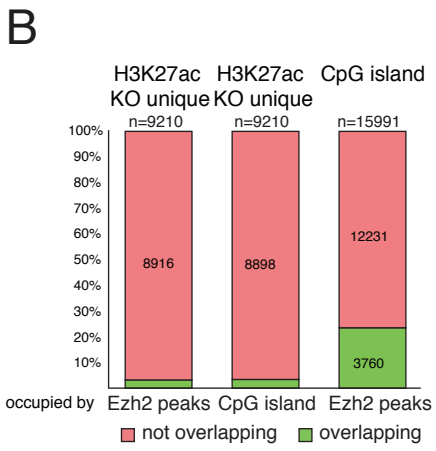
B
H3K27ac KO unique
H3K27ac KO unique
CpG island
n=9210
n=9210
n=15991
8916
8898
12231
3760
occupied by
Ezh2 peaks
CpG island
Ezh2 peaks
not overlapping
overlapping

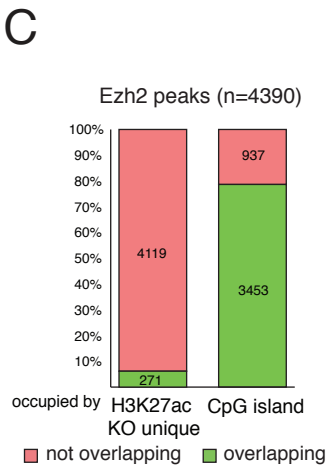
C
Ezh2 peaks (n=4390)
4119
937
3453
271
occupied by
H3K27ac KO unique
CpG island
not overlapping
overlapping

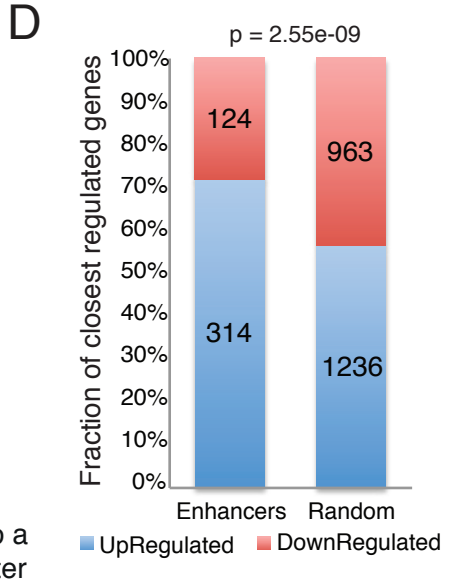
D
p = 2.55e-09
Fraction of closest regulated genes
124
963
314
1236
Enhancers
Random
UpRegulated
DownRegulated

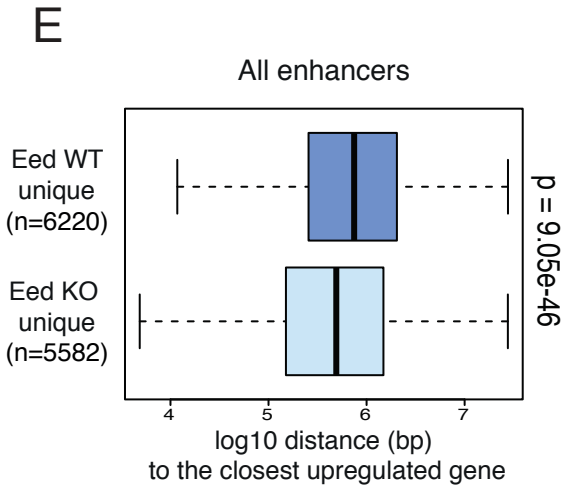
E
All enhancers
Eed WT unique (n=6220)
Eed KO unique (n=5582)
p = 9.05e-46
log10 distance (bp) to the closest upregulated gene

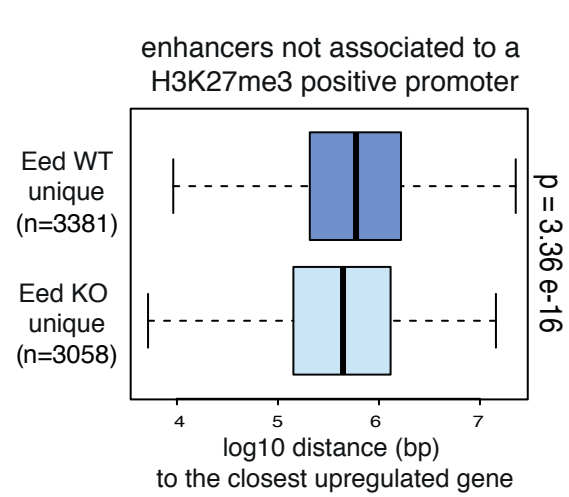
enhancers not associated to a H3K27me3 positive promoter
Eed WT unique (n=3381)
Eed KO unique (n=3058)
p = 3.36 e-16
log10 distance (bp) to the closest upregulated gene

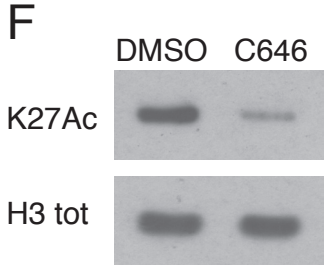
F
DMSO
C646
K27Ac
H3 tot

SUPPLEMENTAL FIGURE AND TABLE LEGENDS

Figure S1. H3K27 methylations are PRC2-dependent. Related to Figures 1-7

(A) Western blot analysis using Eed specific antibody in mouse ES cells expressing scrambled (Ctrl) or *Eed* specific shRNAs. Vinculin served as loading control.

(B) Western blot analyses using H3K36me3 specific antibody of protein extracts prepared from WT (+/+) or *Eed*, *Ezh2* and *Suz12* KO (-/-) mouse ES cell lines or from mouse E14 ES cells expressing scrambled (Ctrl) and *Eed* specific shRNAs. Histone H3 served as loading control.

(C) Quantification of western blot signals for H3K27 methylation forms showed in Figure 1B using ImageJ software. Western blot signal for total histone H3 was used to normalize blot intensities. Reductions in methylation signals upon PRC2 components depletion are expressed as percentage of the normalized blot intensities obtained in wild type (+/+) or control (Ctrl) mouse ES cell lines.

(D) Western blot analysis using antibodies anti-G9a and anti-Glp of protein extracts prepared from mouse ES cells *Eed* WT (Eed +/+), *Eed* KO (Eed -/-) and mouse E14 ES cells simultaneously interfered for *G9a* and *Glp* (G9a/Glp) or unrelated protein (GFP). Vinculin served as loading control.

(E) Western blot analysis using specific H3K27me1, H3K27me2, H3K27me3 antibodies of protein extracts prepared from mouse E14 ES cells interfered for *G9a* and *Glp* or unrelated protein (GFP). Histone H3 served as loading control.

(F) qRT-PCR analyses using primers designed inside (IN) or outside (OUT) of the indicated intragenic loci. ChIP assays were performed in mouse E14 ES cells interfered for *G9a* and *Glp* or unrelated protein (GFP) using indicated specific antibodies. Purified rabbit IgG was a negative control. ChIP enrichments are normalized to histone H3 density. Data represent mean +/- SEM.

(G) Immuno-dot blot analysis showing specificity of the indicated antibodies tested against biotinylated histone H3 peptides bearing specific modification on Lys27. Biotin served as loading control.

(H) Western blot analysis showing H3K27me1 (Upstate) antibody specificity against indicated modified histone H3 peptides.

(I) Cross reactivity screening of the indicated antibodies using a peptide array bearing 384 unique histone modification combinations. Arrows indicate the coordinates on the array of the modified peptide matching the modification to which the antibody avidity is directed. The complete list of spotted peptides is available online at: http://www.activemotif.com/documents/MODified_Histone_Peptide_Array_grid.xls.

(J) Table summarizing data relative to antibody specificity (upper table) and cross-reactivity (lower table) showed in Figure S1I. Coordinates of indicated peptides on the array are shown in brackets. Avidity of antibodies is evaluated on the basis of dot signal intensity.

Figure S2. Inhibition of histone lysine demethylases does not infer on the H3K27 intragenic methylation pattern. Related to Figures 1 and 4.

(A) Relative expression levels of *Utx* and *Jmjd3* determined by qRT-PCR analyses in cells expressing scrambled (Ctrl) or *Utx* and/or *Jmjd3* specific shRNAs (shUtx, shJmjd3 and shUtx + shJmjd3). *Gapdh* served as normalizing expression control. Data represent mean +/- SEM.

(B) Western blot analyses using the indicated antibodies of protein extracts obtained from mouse E14 ES cells stably infected with *Utx*, *Jmjd3* or both specific shRNAs (shUtx, shJmjd3 and shUtx + shJmjd3). A scrambled shRNA sequence was used as negative control (Ctrl). Histone H3 served as loading control.

(C) qRT-PCR of ChIP analyses in mouse E14 ES cells stably infected with *Utx*, *Jmjd3* or both specific shRNAs (shUtx, shJmjd3 and shUtx + shJmjd3) using the indicated antibodies for the indicated regions: Rab7A, Utp6, Fbxl11, Ipo5 are intragenic H3K27me1 enriched regions; promoter region corresponds to the TSS of Wnt5a gene, which is a PRC2 specific target locus; intergenic region corresponds to a H3K27me2 enriched domain. ChIPs with IgG rabbit served as negative control. ChIP enrichments are normalized to histone H3 density. Data represent mean +/- SEM.

(D) Western blot analyses using anti-Hif2 and anti-phospho S6 Ribosomal protein (pS6) specific antibodies of protein extracts obtained from mouse E14 ES cells treated with 100 μM $CoCl_2$ for 48 h. H_2O was used as vehicle control (NT). Total S6 Ribosomal protein served as loading control.

(E) qRT-PCR of H3K27me1 ChIP analyses in mouse E14 ES cells treated with 100 μM $CoCl_2$ for 48 h ($CoCl_2$) or with H_2O (NT). Rab7A, Utp6, Fbxl11, Ipo5 are intragenic H3K27me1 enriched regions; intergenic region corresponds to a H3K27me2 enriched domain. ChIPs with IgG rabbit served as negative control. ChIP enrichments are normalized to histone H3 density. Data represent mean +/- SEM.

Figure S3. Intragenic regions of highly expressed genes are enriched for PRC2-dependent H3K27me1. Related to Figures 2 and 4.

(A) Relative proportion of genes representing the enrichment for either H3K27me1/H3K27me2 within each class of expression generated by RNAseq. High correspond to expression > 3rd quantile; Medium correspond to expression < 3rd and > 1st quantile; Low correspond to expression < 1st quantile.

(B) Average profiles of H3K27me1 and H3K27me2 deposition along the gene bodies (length expressed in %) for all three classes of gene sets shown in A.

(C) Venn diagram showing the number of regulated genes between *Eed* WT mouse ES cell data generated through microarray and mRNA sequencing. P-value was calculated using hypergeometric distribution.

(D) qRT-PCR of ChIP analyses in WT and *Eed* KO mouse ES cells using the indicated antibodies for the loci highlighted by the genomic snapshots shown in the top panels. Primers position respect to the different genomic loci is indicated by the black boxes. Purified rabbit IgG was a negative control. ChIP enrichments are normalized to histone H3 density. Data represent mean +/- SEM.

(E) Overlap between the H3K27me1 enriched genes determined using a Millipore – Upstate anti-H3K27me1 antibody in mouse E14 ES cells (E14) and with the Active Motif anti-H3K27me1 antibody in *Eed* WT (Eed +/+) mouse ES cells. N = 3096 total analyzed genes.

(F) Genomic snapshots of H3K27me1, H3K27me2 and H3K27me3 ChIPseq analyses in WT (Eed +/+) and *Eed* KO (Eed -/-) mouse ES cells together with the results of H3K36me3 ChIPseq analyses from mouse E14 ES cells. H3K27me1 domains are highlighted in blue while H3K27me3 domains are highlighted in red.

Figure S4. PRC2-dependent H3K27me1 deposition is required for correct transcription. Related to Figure 5.

(A) Top left panels show a schematic representation of the GAL4-TK-Luc reporter system of 293Trex cells and the relative difference in Luciferase activity between Gal4-Jarid2 expressing (Gal4-Jarid2) and not expressing cells (Gal4, top right panel). The bottom panels show the qRT-PCR results of ChIP assays from the same cells using the indicated antibodies. Purified rabbit IgG was a negative control. ChIP enrichments are normalized to histone H3 density for H3K27me1, H3K27me3 and H3K36me3, while Gal4 ChIP enrichments are presented as percentage (%) of bound/input signal. The black arrows indicate the position of the qRT-PCR primers relative to the GAL4-TK-Luc construct. Data represent mean +/- SEM.

(B) Relative expression of the indicated differentiation markers determined by qRT-PCR in WT and *Eed* KO mouse ES cells before (ES) and after (EB) differentiation. Gene expression is normalized to *Gapdh* levels. Data represent mean +/- SEM.

(C) The left panel shows the average profiles of H3K27me1 deposition along the bodies (length expressed in %) of the subset of genes (~50%) shown in Figure 5E that are differentially activated (1.5 fold difference) between Eed WT and KO EBs. The right panel shows the expression levels of the same genes in ES and EBs WT and KOs for Eed. p-value was calculated with Wilcoxon test.

Figure S5. Setd2-dependent H3K36me3 controls PRC2 enzymatic activity *in vivo*. Related to Figure 6.

(A) Venn plot of down regulated genes between WT/*Eed* KO mouse ES cells and shCtrl/shSetd2 KD. P-value was calculated using hypergeometric distribution.

(B) Confocal immunofluorescence images of mouse E14 ES cells expressing scrambled (shRNA Ctrl) or *Setd2* specific shRNAs (shRNA Setd2) 3 h after release in presence of BrdU after a 12 h long thymidine block, stained with the indicated antibodies. Bar plots indicate the average Mender's co-localization coefficient among all Z-stacks for each cell. Error bars indicate SD. p-value is calculated by student t-test. Data represent mean +/- SEM.

(C) Extract ion chromatograms relative to (27-40) KSAPSTGGVKKPHR peptide from unmodified recombinant histone H3 (H3 Histone) and recombinant histone H3 with K36me3 (H3Kc36me3 Histone) and estimation of relative percentage species (RS%). In the upper panel: extract ion chromatograms of precursor ions corresponding to the recombinant H3 (27-40) peptide upon enzymatic reaction were identified as unmodified (K27me0), mono- (K27me1) and di-methylated (K27me2) on K27 and depicted in blue, red and green, respectively (H3 Histone + PRC2). Extract ion chromatograms of the same peptide in absence of enzyme was also reported as a control (H3 Histone). In the lower panel: extract ion chromatograms of precursor ions of recombinant

H3Kc36me3 (27-40) peptide upon enzymatic reaction (H3Kc36me3 Histone + PRC2)**.** Extract ion chromatograms of the same peptide in absence of enzyme was also reported as a control (H3Kc36me3 Histone)**.** In each case relative species percentage (RS%) (see Material and Method), was also displayed in bar plot. Shift in retention time among the different degree of modification is due to D3-acetyl chemical alkylation on lysine residues.

(D) Coomassie staining of histone proteins extracted from mouse E14 ES cells before and after enrichment by immunopurification with anti-H3K36me3 specific antibody.

(E) Annotated MS/MS spectrum of modified (27-40) KSAPSTGGVKKPHR peptide from H3.3 generated from the fragmentation of the precursor ion with m/z 790.4811 and charge +2 assigned to the tetra-methylated form of peptide H3.3 (27-40), upon chemical modification (D3-acetylation) reveals coexistence of mono-methylated K27 and tri-methylated K36 within the same peptide. Uniprot accession number, score and posterior error probability (PEP) relative to peptide identification by MaxQuant are reported in the left panel.

(F) Annotation of product ions from CID fragmentation of tetra-methylated and D3-acetylation peptide (27-40) KSAPSTGGVKKPHR from H3.3. The table summarizing the b- and y- ions produced by CID-fragmentation is reported, as generated by Viewer.exe software. The b- and y-ions experimentally detected are reported in blue and red, respectively. Mass deviation for each experimental ion in the fragmentation spectrum is less than 0.5 Da (bottom left panel). The different modification upon *in vitro* D3-acetyl alkylation and the corresponding ΔM that were specified as variable modifications in Andromeda Search Configuration are annotated (bottom right panel).

Figure S6. Loss of H3K27me2 disrupts canonical ES-specific enhancer regulation. Related to Figure 7.

(A) qRT-PCR analyses of DNA purified from H3K27ac ChIP in WT and *Eed* KO mouse ES cells using primers amplifying the indicated genomic loci. Chromosomal coordinates correspond to the

center of the amplified genomic region. Purified rabbit IgG was a negative control. ChIP enrichments are normalized to histone H3 density. Data represent mean +/- SEM.

(B) Genomic snapshots of ChIPseq analyses using H3K27me1, H3K27me2, H3K27me3, H3K27ac, H3K4me1 and H3K4me3 specific antibodies in WT (Eed +/+) and *Eed* KO (Eed -/-) mouse ES cells. Regions of regulated H3K27ac are highlighted in yellow as in Figure 7C.

(C) Boxplot quantifying the H3K4me3 and H3K27me3 intensity in the unique H3K27ac distal peaks of Eed WT and Eed KO samples (shown in Figure 7D). Eed WT unique peaks; n=12341. Eed KO unique peaks; n=9210.

Figure S7. Enhancer deregulation induced by PRC2 deficiency correlates with gene activation. Related to Figure 7.

(A) Comparative analysis on the levels of H3K27me3, H3K27ac, H3K4me1, and H3K4me3 in the regions of active enhancers, promoters with H3K27me3 positive and poised enhancers between Human (Rada-Iglesias et al., 2011) and mouse ES samples. Left and middle panel represents classification of human enhancers on the basis of p300 occupancy or H3K4me1 enrichment. The right panel represents the classification of mouse enhancers on the basis of H3K4me1 enrichment. p300 based human enhancers: active n=5118; poised n=2287; K27me3 positive promoters n=6451. Human enhancers classified respect to H3K4me1 deposition: active n=10807; poised n=27032; K27me3 positive promoters n=6451. Mouse enhancers classified respect to H3K4me1 deposition: active n=8445; poised n=36046; K27me3 positive promoters n=4386.

(B) Left and middle bars: percentage of Ezh2 peaks occupancy (determined by ChIPseq analysis in mouse E14 ES cells) and of CpG islands respect to genomic regions corresponding to H3K27ac peaks uniquely found in *Eed* KO mouse ES cells. Right bar: percentage of Ezh2 peaks respect to genomic regions corresponding to CpG islands. n = numbers of peaks.

(C) Relative occupancy of H3K27ac peaks uniquely found in *Eed* KO mouse ES cells (left bar) and of CpG islands (right bar) relative to genomic regions corresponding to EZH2 peaks determined by ChIPseq analysis in E14 mouse ES cells. n = numbers of peaks.

(D) Bar plot showing preferential enrichment of up-regulated genes associated with Eed KO active enhancers with respect to genome wide random dataset. p-value is computed by chi-square analysis.

(E) Representation of the relative distance between putative WT and Eed KO enhancers and the up-regulated genes in Eed KO ES cells. In the top panel all identified enhancers are included in the analysis. The bottom panel represents the same analysis in which the enhancers associated to an H3K27me3 positive gene in WT ES cells were excluded from the analysis. H3K27me3 enriched genes were defined by the presence of a H3K27me3 peak within +/- 2.5kb from the TSS. p-values were calculated by Mann-Whitney Test.

(F) Western blot analysis for H3K27ac antibody of protein extracts prepared from mouse E14 ES cells treated with 35 μM C646 p300 inhibitor for 48 h. DMSO was used as vehicle control. Histone H3 served as loading control.

Table S1. Related to Figures 2,4,5 and 7.

Sheet 1: Enrichment values of different histone PTMs for all RefSeq genes in mouse E14 ES cells. Sheet 2: Genes expression analyses in WT and *Eed* KO mouse ES cells. Sheet 3: Enrichment values of histone H3 and H3K27me1 for all RefSeq genes in WT and *Eed* KO mouse ES cells. Sheet 4: List of H3K27ac peaks identified in WT and *Eed* KO mouse ES cells with RefSeq TSS annotation.

Table S2. Related to Figures 4-6

List of sequences for the Real-Time quantitative PCR primer pairs.

SUPPLEMENTAL EXPERIMENTAL PROCEDURES

Tissue culture

All mouse ES cell lines were grown on 0.1% gelatinized tissue culture dishes in GMEM supplemented with 15% fetal calf serum (Euroclone), 2 mM glutamine (Gibco), 100 U/ml penicillin and 0.1 mg/ml streptomycin (Gibco), 0.1 mM non-essential amino acids (Gibco), 1 mM Na-pyruvate (Gibco), 50 µM ß-mercaptoethanol-phosphate-buffered saline (PBS; Gibco) and leukemia inhibitory factor (LIF) (produced in house). *Ezh2* conditional (loxP/loxP) mouse ES cells, *Eed* WT and KO mouse ES cells, and *Suz12* KO mouse ES cells were described previously (Pasini et al., 2007; Pasini et al., 2010; Schoeftner et al., 2006).

Gal4-Jarid2-inducible 293Trex cells are described elsewhere (Pasini et al., 2010). The expression of Gal4-Jarid2 was induced by the addition of 1 µg/ml doxycycline (Sigma) to the cell media for 48 hr before collecting for luciferase and ChIP analyses. Cell lysates were prepared with passive lysis buffer (Promega) and processed for the Bradford protein assay (Biorad) and the luciferase assay (Promega) according to the manufacturer's protocol.

Where indicated, WT mouse ES cells were treated with 100 µM $CoCl_2$ (Sigma Aldrich) for 48 hr. H_2O was used as a vehicle control.

Histone acetylation was inhibited by treating WT mouse ES cells with 35 µM C646 p300 inhibitor (EMD Millipore, Cat. 382113) for 48 hr. DMSO was used as a vehicle control.

RNA interference

Stable shRNA knock downs were obtained with mouse ES cell transduction using viral particles produced with the pLKO.1 vectors TRCN0000238533 (shSetd2), TRCN0000095719 (shEed), TRCN0000096242 (shUtx), TRCN0000095265 (shJmjd3), and SHC202 (shSCR), purchased from Sigma-Aldrich, as described elsewhere (Vella et al., 2011). Endoribonuclease-prepared siRNA (esiRNA) Glp (EMU068911), esiRNA G9a (EMU050951), and esiRNA GFP (EHUEGFP) were purchased from Sigma-Aldrich and transfected into E14 mouse ES cells using Lipofectamine 2000 (Invitrogen).

EB formation

Differentiation experiments were performed as described previously (Pasini et al., 2007; Pasini et al., 2010). Undifferentiated ES cells were induced to differentiate into embryoid bodies (EBs) by LIF removal in hanging drops containing 1000 cells / 20 µl drop on the lid of 15 cm petri dishes for 48 hr. EBs were then collected from the drops and stimulated between days 2 and 5 with 0.5 µM all-trans-retinoic acid (ATRA). EBs were left in culture in non-coated petri dishes until up to day 9 in ES medium without LIF. Medium was replaced every second day.

Antibodies

Immunoblotting, FACS, and chromatin immunoprecipitation (ChIP) analyses were performed with the following antibodies: rabbit anti-H3 (Abcam, Cat. 1791), rabbit anti-H3K27me1 (Upstate, Cat. 07-448), mouse anti-H3K27me1 (Active Motif, Cat. 61015), rabbit anti-H3K27me2 (Cell Signaling, Cat. 9728), rabbit anti-H3K27me3 (Active Motif, Cat. 39155), rabbit anti-H3K27ac (Abcam, Cat. 4729), rabbit anti-H3K27ac (Active Motif, Cat. 39133), rabbit anti-H3K36me3 (Cell Signaling, Cat. 4909), rabbit H3K4me1 (Abcam, Cat. 8895), rabbit anti-H3K4me3 (Active Motif, Cat. 39159), mouse anti-vinculin (Sigma-Aldrich, Cat. V9131), rabbit anti-GAL4 (Santa Cruz, Cat. Sc-577), rabbit anti-Hif2 (Novus Biologicals, Cat. NB 100-122), mouse anti-S6 Ribosomal protein (Cell Signaling, Cat. 2317), rabbit anti-phospho S6 Ribosomal protein (Cell Signaling, Cat. 4857), rabbit anti-G9a (Cell Signaling, Cat. 3306S), rabbit anti-Glp (Abcam, Cat. 41969), and mouse anti-Eed, as described elsewhere (Pasini et al., 2004). Rabbit IgG (Sigma, Cat. I5006) was used as a negative control in ChIP and immunoprecipitation experiments.

For immunofluorescence staining, the following antibodies were employed: rabbit anti-Suz12 (Cell Signaling, Cat. 3737S), mouse anti-BrdU (BD Biosciences, Cat. 347580), Alexa fluor 488 conjugated donkey anti-rabbit (Invitrogen, Cat. A21206), and FITC conjugated donkey anti-mouse (Jackson Immunoresearch, Cat. 715095150).

Antibody Specificity test

Antibody specificity for mouse anti-H3K27me1 (Active Motif, Cat. 61015), rabbit anti-H3K27me2 (Cell Signaling, Cat. 9728), rabbit anti-H3K27me3 (Active Motif, Cat. 39155), rabbit anti-H3K4me1 (Abcam, Cat. 8895), rabbit anti-H3K36me3 (Cell Signaling, Cat. 4909) was tested by immunoblot on a MODified™ Histone Peptide Array (Active Motif, Cat. 13005) according to manufacturer's instructions.

Mouse anti-H3K27me1 (Active Motif, Cat. 61015), rabbit anti-H3K27me2, and rabbit anti-H3K27me3 were further tested by immuno-dot blot assay, spotting 1 µg of biotinylated histone H3 peptides, non-methylated, mono-, di-, or tri-methylated on lys27 (JPT Peptide Technologies GmbH, custom made) on a nitrocellulose membrane, then analyzed by Western blot. Biotin was used as a loading control.

Rabbit anti-H3K27me1 (Upstate, Cat. 07-448) was tested by Western blot against 1 µg of the indicated H3 peptides run on a polyacrylamide gel.

Cell cycle analysis and flow cytometry

To assess antibody specificity, *Eed* WT and KO mouse ES cells were stained first with H3K27me2 antibody (Cell Signaling, Cat. 9728) and unrelated rabbit IgG as isotype control, then with APC-conjugated secondary antibody. Cell events were acquired with a FACSCalibur flow cytometer (BD Biosciences) and analyzed with FlowJo 8.5.3 software (Tree Star). For cell cycle analysis, E14 mouse ES cells were cultured as previously described and pulsed with 33 µM 5-bromo-2-deoxyuridine (BrdU) for 15 min. Cells were washed with PBS, fixed with 75% ethanol, denatured with 2N HCl, and neutralized by 0.1 M Borax. Cell staining was performed in blocking buffer solution using mouse anti-BrdU and rabbit anti-H3K27me2 as primary antibodies, and anti-mouse IgG-FITC conjugate and anti-rabbit IgG-APC conjugate were used as secondary antibodies. Cells were finally re-suspended in PBS containing 2.5 µg/ml propidium iodide in the presence of RNase A and analyzed with FACSCalibur flow cytometer (excluding doublets and non-viable cells). Collected data were analyzed with Cell Quest Pro (BD Biosciences), and the single-cell

fluorescence intensity values of the gated populations were retrieved using FCS Assistant software.

Non-nucleosomal histone H3 enrichment

Whole cell extracts from E14 mouse ES cells were obtained by swelling cell pellets in high salt lysis buffer (20 mM Tris-HCl, pH 7.6, 300 mM NaCl, 10% glycerol, 0.2% (v/v) Igepal (Sigma-Aldrich, Cat. CA 630), which were then incubated for 30 min on ice and centrifuged at 13 000rpm for 30 min at 4°C. To enrich soluble histones, 1 mg of total extract was incubated overnight with 3 µg of rabbit anti-histone H3 antibody on a rotating platform at 4°C. Immunoprecipitated proteins were recovered by addition of 30 µL protein A-sepharose beads (GE Healthcare) for 1 hr at 4°C. Beads were washed six times with lysis buffer, and samples were denatured in Laemmli sample buffer for 5 min at 95°C, loaded on a polyacrylamide gel, and analyzed by Western blot.

Immunofluorescence

Mouse E14 ES cells interfered for Setd2 protein and scrambled control were seeded on 0.1% gelatinized glass coverslip and synchronized in G1/S phase by addition of 2 mM thymidine for 12 hr. After 3 hr release in normal medium, the cultured cells were pulsed with 33 µM BrdU for 30 min. Nuclei on coverslips were prepared by treatment with cold pre-extraction buffer (10 mM Tris HCl, pH 7.6, 100 mM NaCl, 2 mM $MgCl_2$, 0,3 M sucrose, and 0.25% Igepal) for 10 min at 4°C. Nuclei were fixed at –20°C with 100% methanol for 10 min and further incubated with 20 mU/µl of DNAse I (NEB) for 30 min at 37°C to unmask incorporated BrdU. Fixed nuclei were then incubated with primary antibodies diluted in 0.1% Tween-TBS for 1 hr at RT, washed, and incubated with fluorophore-conjugated secondary antibodies. Nuclei were counterstained with DAPI and embedded in anti-fade–containing glycerol (DABCO).

Images were acquired using a Leica SP2 confocal microscope. Mender's co-localization coefficient was calculated on the entire Z-stacks images using the jacop tool of the Image J software.

ChIP and ChIP-sequencing

ChIP assays were carried out as described previously (Pasini et al., 2010). Briefly, 1% formaldehyde cross-linked chromatin was fragmented by sonication to an average size of 200–400bp and incubated overnight in IP Buffer (33 mM Tris/HCl, pH 8, 100 mM NaCl, 5 mM EDTA, 0.2% NaN3, 0.33% SDS, 1.66% Triton X-100) at 4 ºC with 1–5 µg of the indicated antibodies, followed by incubation for 2–4 hr with protein A sepharose beads (GE Healthcare). Beads were washed three times with 150 washing buffer (20 mM Tris/HCl, pH 8, 150 mM NaCl, 2 mM EDTA, 0.1% SDS, 1 % Triton X-100), once with 500 washing buffer (20 mM Tris/HCl, pH 8, 500 mM NaCl, 2 mM EDTA, 0.1% SDS, 1% Triton X-100), and finally re-suspended in 120 µl of de-crosslinking solution (0.1 M NaHCO3, 1% SDS). For ChIP-seq, the DNA from a ChIP experiment was prepared with the Illumina ChIPSeq sample prep kit (IP-102-1001) and multiplexing oligonucleotide kit (PE-400-1001) by our internal genomic facility. DNA libraries were quantified using a high sensitivity Chip on Bioanalyzer (by Agilent) and used for cluster generation and sequencing using the HiSeq 2000 (Illumina) following the manufacturer's protocol.

RNA sequencing

Total RNAs from mouse ES cell lines and embryoid bodies were extracted using TRIzol reagent (Invitrogen, Cat. 15596) according to the manufacturer's instructions. Retrieved RNA was then converted into libraries of double-stranded cDNA suitable for next generation sequencing on the Illumina platform, using the Illumina TruSeq v.2 RNA sample preparation kit according to manufacturer's recommendations. Briefly, mRNA was purified from 5 µg of total RNA using poly-T oligo-attached magnetic beads and then fragmented using divalent cations contained in the Illumina fragmentation buffer and high temperatures. First, cDNA strand was synthesized with random oligos by Reverse Transcriptase SuperScript III (Invitrogen). Next, cDNA strand synthesis was performed by DNA polymerase I and RNase H. Finally, DNA fragments were blunt ended and adenylated at 3′ extremities before ligating to specific Illumina oligonucleotides adapters. The resulting fragments were enriched by 15 cycles of PCR reaction using proprietary Illumina primer mixes. Prepared libraries were quality checked and quantified using Agilent high-sensitivity DNA assay on a Bioanalizer 2100 instrument (Agilent Technologies).

Sequencing and expression data analysis

Sequencing data generated from the Illumina platforms were aligned to mouse reference genome (mm9) using Bowtie version 0.12.7. Only reads with unique alignment were retained for downstream analysis. Peak calling and bigWig files were generated using MACS version 1.4. Only peaks with 10x-Log p-value ≥70 are considered for further processing. bigWig files were visualized using the UCSC browser (http://genome.ucsc.edu). The list of mm9 annotated RefSeq genes used for the different analyses was downloaded from the UCSC database.

RNASeq data generated for ES WT, ES Eed KO, Ebs WT, Ebs Eed KO samples were aligned to mouse reference genome using tophat. Differentially expressed genes were identified with cuffdiff. Microarray raw data were retrieved from the Gene Omnibus Database (http://www.ncbi.nlm.nih.gov/geo/) at the accession number GSE19076. Data were RNA normalized using the affy package in R and probeset with a >1.3 fold change (FC) difference and a 95% confidence determined by T-test were selected for the analyses.

Intragenic reads density for histone H3, H3K27me1, H3K27me2 and H3K36me3 were determined by computing the count of aligned reads within each RefSeq genes normalized for sequencing depth. PTM enrichments relative to histone H3 density were determined for each gene as the 10x–Log p-value computed using a chi-square test (PTM vs. H3) and adjusted using Bonferroni correction. The corrected p-values between different PTMs were compared using Pearson correlation test. Genome wide correlation among H3K27me1, H3K27me2 and H3K36me3 modifications with the corrected p-values generated for all gene bodies were subjected to both local and global analysis. Local analysis refers to the state of occupancy of any two modifications at a given instant over all coding genes (RefSeq) or to the indicated loci. This is achieved by computing pairwise correlation between all possible pairs of PTMs through scatter plot and further fitting lowess regression model over the data. The strength of the trend was further confirmed by correlation coefficient computed through pearson correlation test. Global analysis takes into consideration all PTMs together. This is achieved through Principle Component Analysis (PCA). To determine the relation between different PTMs, we choose principal components 1 and 2, which

was able to cover 90 percent variation of data. The extent of correlation between PTMs was computed through factor analysis approach. All statistical analyses were performed in R and PCA was performed using factorMineR package. Genes were classified on the basis of their expression levels distribution. We considered genes with expression levels greater than third quantile as highly expressed genes, genes with expression levels less than first quantile as low expressed genes and others in between as medium expressed genes. For generating the average occupancy in gene bodies, the gene body of each RefSeq gene was split into 20 bins where each bin represents 5% of the gene length. The occupancy was computed in each bin, normalized to the length of the bin and to the sequencing depth and then averaged over all genes. Intensity of each modification in all set of classes was then scaled down to a 0 to 1 range.

TSS vs. non-TSS location of H3K27ac peaks was determined by overlapping H3K27ac peaks with a 5 kb region centered on TSS for each mm9 RefSeq annotated gene. For capturing real intensities at the sites of active enhancers marked by K27ac peaks distal from TSS in comparison with genome wide distribution, we partitioned genome into small non-overlapping bins of 500 bp in size. Within these regions the histone H3 modifications K27ac, K4me1, K4me3, K27me3 and K27me2 from both WT and Eed KO samples were quantified by counting the number of aligned reads in the regions followed by sequencing depth normalization and adjustment of outlier values to 99th quintile. Further for reducing background levels specifically for K27me2 in Eed KO as compared to WT samples we applied a normalizing factor quantified through chip experiments to the intensities in both WT and Eed KO samples. The intensities generated using the same antibody in WT and Eed KO samples were then scaled down to a 0 to 1 range. Finally, the bins overlapping with K27ac distal peaks were merged together and the intensities obtained for all modifications between WT and Eed KO samples were represented as heatmap.

Each H3K27ac KO distal peak was assigned to the closest TSS RefSeq gene. These genes were then classified accordingly to their expression levels between WT and Eed KO and classified as up regulated (FC > 3) or down-regulated (FC < 3). For the genes belonging to each class as well as in the entire RNASeq dataset, we determined if the observed frequencies of up-regulated and down-

regulated genes under putative control of the H3K27ac distal peaks were significantly different respect to the expected frequencies determined by analyzing the whole RNAseq dataset. Accordingly, we determined the relative distance of each H3K27ac distal peak identified in either WT or Eed KO samples respect to the closest up-regulated gene in Eed KO ES cells.

Active enhancers were classified on the basis of presence of both H3K27ac and H3K4me1 peaks, the absence of H3K4me3 and a minimal distance of 2.5Kb from annotated TSSs. Poised enhancers were defined by the absence of H3K27ac using the same criteria. The relative intensities of all the indicated histone marks were determined at H3K27me3 positive promoters, at poised and at active enhancers in both human and mouse ES cells. For human ES cells we used previously published ChIPseq data (Creyghton et al., 2010; Rada-Iglesias et al., 2011).

Real-time quantitative PCR and primers

Total RNA was extracted with the Qiagen RNeasy Plus RNA extraction kit and retro-transcribed with M-MuLV Reverse Transcriptase RNase H (Finnzyme) according to the manufacturer's instructions. Real-time quantitative PCR (qPCR) was carried out using Fast Sybergreen as previously described (Pasini et al., 2008) and performed following the manufacturer's instructions (Applied Biosystems). The analysis of the results was performed as described previously (Pasini et al., 2008). Primers sequences are available upon request.

***In vitro* methyltransferase assay**

In vitro histone methyltransferase assays were performed by incubating 0.5 µg recombinant MLA histone H3K36me3 (Active Motif, Cat. 31219) or recombinant non-modified histone H3 (Active Motif, Cat. 31207) with 1.5 µg human recombinant PRC2 complex (Sigma Aldrich, Cat. SRP0134) in 50 mM TRIS HCl, pH 8.6, 5 mM $MgCl_2$, 4 mM DTT, and 20 µM S-adenosylmethionine (New England Biolabs, Cat. B9003). Reactions were performed at 30°C for 1 hr, then blocked with Laemmli sample buffer (Invitrogen) and denatured for 5 min at 95°C. Samples were loaded on a 4–12% NuPAGE Novex Bis-Tris gel (Invitrogen) to separate histones in order to perform subsequent in-gel digestion for MS analysis.

Acidic extraction of histones and Immunopurification

Mouse E14 ES cells were harvested, resuspended in N-Buffer (15 mM HEPES, pH 7.5, 10% sucrose, 0.5% Triton X-100, 0.5 mM EGTA, 60 mM KCl, 15 mM NaCl, 30 µg/ml Spermine, 30 ug/ml Spermidine, 1 mM DTT, 3 mM NaButyrate, 5 mM NaF, 5 mM Na-Pyrophosphate, 5 mM ß-glycerophosphate) with fresh addition of a protease inhibitor cocktail (Calbiochem) at a cell density of 125×10^6 cells/ml and lysed 10 min at 4ºC with gentle stirring. Lysate was centrifuged onto a 10% sucrose cushion (10^7 cells/cushion) at 4000 rpm for 30 min and washed twice in ice cold 1× PBS. Histones were extracted in 0.4 N HCl overnight at 4ºC with gentle stirring, extensively dialyzed in 0.1 M acetic acid, and dried out. Histone pellets were re-suspended in histone buffer (50 mM Tris/HCl, pH 8.0, 150 mM NaCl, 5 mM EDTA, 1% Triton X-100) and incubated at 4ºC for 4 hr with 10 µg of H3K36me3 antibody followed by a 3 hr incubation with protein A-sepharose beads (GE Healthcare). Beads were washed twice in 10–20 × bead volumes with histone buffer and twice in 1× PBS, and then eluted in Laemmli sample buffer (Invitrogen).

In-gel digestion of histones for MS analysis

Immunopurified sample was separated by 1D SDS-PAGE, using 4–12% NuPAGE® Novex Bis–Tris gels (Invitrogen) and NuPAGE® MES SDS running buffer (Invitrogen), according to the manufacturer's instructions. The gel was stained with Coomassie Blue using Colloidal Blue Staining Kit (Invitrogen). The protein band corresponding to immunopurified histone H3 was excised from the gel, de-stained with 50% acetonitrile (MeCN) diluted in H_2O, and then chemically alkylated by incubation with acetic anhydride-D6 (Sigma 175641) in a 1:9 ratio in 1M NH_4HCO_3, as previously described (Bonaldi et al., 2004). After 3 hr at 37°C with strong shaking (1400 rpm), gel pieces were washed with increasing concentrations of MeCN. In-gel digestion was performed with 7.5 ng/ml trypsin (Promega V5113) in 50 mM NH_4HCO_3 at 37°C overnight. The supernatant was transferred to a fresh tube, and the remaining peptides were extracted by incubating gel pieces twice with 30% MeCN in 3% trifluoroacetic acid (TFA), followed by dehydration with 100% MeCN. The extracts were pooled, reduced in volume in a vacuum concentrator, desalted and concentrated using a combination of in-house–made RP-C_{18}/Carbon and a strong cation exchange (SCX) solid

phase extraction (SPE) StageTip (Rappsilber et al., 2007). Briefly, digested peptides loaded on combined RP-C_{18}/Carbon and SCX StageTip were eluted with high organic solvent (80% MeCN) and NH_4OH, respectively. Eluted peptides were lyophilized, re-suspended in 0.1% TFA and 0.5% acetic acid in ddH_2O, pooled, and subjected to LC-MS/MS.

Liquid Chromatography and Tandem Mass Spectrometry (LC-MS/MS)

Peptide mixtures were separated by nano-liquid chromatography using an EASY-nLC system (Proxeon Biosystems, Odense, Denmark) connected to the hybrid dual-pressure linear ion trap/orbitrap mass spectrometer (LTQ Orbitrap Velos, Thermo Scientific). The nanoliter flow LC was operated in one column set-up with a 15 cm analytical column (75 µm inner diameter, 350 µm outer diameter) packed with C18 resin (ReproSil, Pur C18AQ 3 µm, Dr. Maisch, Germany). Solvent A was 0.1% FA and 5% ACN in ddH_2O ,and solvent B was 95% ACN with 0.1% FA. Separation was performed with a gradient of 0–40% solvent B over 90 min, followed by a gradient of 40–60% for 10 min and 60–80% over 5 min at a flow rate of 250 nl/min. The LTQ Orbitrap Velos MS was used in the data-dependent mode. CID-fragmentation method when acquiring MS/MS spectra consisted of an orbitrap full MS scan followed by up to 20 LTQ MS/MS experiments (TOP20) on the most abundant ions detected in the full MS scan. Essential MS settings were as follows: full MS (AGC 1,000,000; resolution 30,000; m/z range 300-1500; maximum ion time 500 ms); MS/MS (AGC 30,000; maximum ion time 100 ms; minimum signal threshold 500; isolation width 2 Da; dynamic exclusion time setting 30 s (±10 ppm relative to the precursor ion m/z); singly charged ions and ions for which no charge state could be determined were excluded from selection. Normalized collision energy was set to 35%, and activation time to 10 ms; spray voltage, 2.2 kV; no sheath and auxiliary gas flow; heated capillary temperature, 275ºC; predictive automatic gain control (pAGC) enabled, and an S-lens RF level of 65%. For all full-scan measurements with the Orbitrap detector, a lock mass ion from ambient air (m/z 445.120024) was used as an internal calibrant as described previously (Olsen et al., 2005).

Data Analysis and Peptide Assignment by MaxQuant

The mass spectrometric raw data were analyzed with the MaxQuant software (version 1.1.1.25) (Cox et al., 2009). A false discovery rate (FDR) of 0.01 for proteins and peptides, and a minimum peptide length of 6 amino acids, were required. In order to improve mass accuracy of the precursor ions, the time-dependent recalibration algorithm of MaxQuant was used (Cox and Mann, 2008). The MS/MS spectra were searched by Andromeda engine against the IPI human database (containing 87,061 entries) combined with 262 common contaminants and concatenated with the reversed versions of all sequences (Cox et al., 2011). Enzyme specificity was set to Arg-C and maximum of three missed cleavages were allowed. Peptide identification was based on a search with an initial mass deviation of the precursor ion of up to 7 ppm. The fragment mass tolerance was set to 20 ppm on the m/z scale. Variable modifications included: deuterate acetylation (D3-acetylation) (+45.0294 Da) on lysine, lysine mono-methylation (calculated as the sum of the masses of D3-acetylation (+45.0294) and mono-methylation (+14.016 Da)), dimethylation (+ 28.031 Da) and tri-methylation (42.046 Da), lysine acetylation (+ 42.010 Da), methionine oxidation (+ 15.995 Da) and N-terminal protein acetylation. D3-acetyl chemical alkylation results in a delta mass of 45.0294 Da for each group added either to the unmodified or mono-methylated Lysine, allowing the discrimination of isobaric modified peptides (Bonaldi et al., 2004; Garcia et al., 2007; Loyola et al., 2006). Output table from MaxQuant were filtered with the following criteria: peptides with a low score (cut-off score value, 60) (Thakur et al., 2011) and with more than 5 putative PTMs per peptide were removed. Redundant peptides were filtered so that only the peptide with the highest Andromeda score among peptides with the same identification was included. The filtered data were then subjected to manual validation using Qual Browser version 2.2 (ThermoFisher Scientific). Estimation of relative species percentage (RS%) calculated extracted ion chromatograms (XIC) were constructed for precursor ions with mass tolerance of 10 ppm and mass precision up to 4 decimal places using Qual Browser version 2.2. Peak areas for both unmodified and modified peptide species were measured within the same retention time interval.

Relative species percentage (RS%) for (27–40) peptides both from H3(C110A) and H3(MLA) was calculated dividing the peak area relative to each peptide species divided by the sum of peak areas

for all peptide species sharing the same amino acid sequence. Specific delta masses relative to modified sequence of (27–40) peptides from H3(MLA) was further included in Andromeda configuration module (AndromedaConfig.exe); for the specific delta masses, we referred to manufacturer specification (http://www.activemotif.com/).

SUPPLEMENTAL REFERENCES

Bonaldi, T., Regula, J.T., and Imhof, A. (2004). The use of mass spectrometry for the analysis of histone modifications. Methods in enzymology *377*, 111-130.

Cox, J., and Mann, M. (2008). MaxQuant enables high peptide identification rates, individualized p.p.b.-range mass accuracies and proteome-wide protein quantification. Nature biotechnology *26*, 1367-1372.

Cox, J., Matic, I., Hilger, M., Nagaraj, N., Selbach, M., Olsen, J.V., and Mann, M. (2009). A practical guide to the MaxQuant computational platform for SILAC-based quantitative proteomics. Nature protocols *4*, 698-705.

Cox, J., Neuhauser, N., Michalski, A., Scheltema, R.A., Olsen, J.V., and Mann, M. (2011). Andromeda: a peptide search engine integrated into the MaxQuant environment. Journal of proteome research *10*, 1794-1805.

Garcia, B.A., Mollah, S., Ueberheide, B.M., Busby, S.A., Muratore, T.L., Shabanowitz, J., and Hunt, D.F. (2007). Chemical derivatization of histones for facilitated analysis by mass spectrometry. Nature protocols *2*, 933-938.

Loyola, A., Bonaldi, T., Roche, D., Imhof, A., and Almouzni, G. (2006). PTMs on H3 variants before chromatin assembly potentiate their final epigenetic state. Molecular cell *24*, 309-316.

Olsen, J.V., de Godoy, L.M., Li, G., Macek, B., Mortensen, P., Pesch, R., Makarov, A., Lange, O., Horning, S., and Mann, M. (2005). Parts per million mass accuracy on an Orbitrap mass spectrometer via lock mass injection into a C-trap. Molecular & cellular proteomics : MCP *4*, 2010-2021.

Pasini, D., Bracken, A.P., Hansen, J.B., Capillo, M., and Helin, K. (2007). The polycomb group protein Suz12 is required for embryonic stem cell differentiation. Mol Cell Biol *27*, 3769-3779.

Pasini, D., Bracken, A.P., Jensen, M.R., Lazzerini Denchi, E., and Helin, K. (2004). Suz12 is essential for mouse development and for EZH2 histone methyltransferase activity. The EMBO journal *23*, 4061-4071.

Pasini, D., Cloos, P.A., Walfridsson, J., Olsson, L., Bukowski, J.P., Johansen, J.V., Bak, M., Tommerup, N., Rappsilber, J., and Helin, K. (2010). JARID2 regulates binding of the Polycomb repressive complex 2 to target genes in ES cells. Nature *464*, 306-310.

Pasini, D., Hansen, K.H., Christensen, J., Agger, K., Cloos, P.A., and Helin, K. (2008). Coordinated regulation of transcriptional repression by the RBP2 H3K4 demethylase and Polycomb-Repressive Complex 2. Genes Dev *22*, 1345-1355.

Rada-Iglesias, A., Bajpai, R., Swigut, T., Brugmann, S.A., Flynn, R.A., and Wysocka, J. (2011). A unique chromatin signature uncovers early developmental enhancers in humans. Nature *470*, 279-283.

Rappsilber, J., Mann, M., and Ishihama, Y. (2007). Protocol for micro-purification, enrichment, pre-fractionation and storage of peptides for proteomics using StageTips. Nature protocols *2*, 1896-1906.

Schoeftner, S., Sengupta, A.K., Kubicek, S., Mechtler, K., Spahn, L., Koseki, H., Jenuwein, T., and Wutz, A. (2006). Recruitment of PRC1 function at the initiation of X inactivation independent of PRC2 and silencing. The EMBO journal *25*, 3110-3122.

Thakur, S.S., Geiger, T., Chatterjee, B., Bandilla, P., Frohlich, F., Cox, J., and Mann, M. (2011). Deep and highly sensitive proteome coverage by LC-MS/MS without prefractionation. Molecular & cellular proteomics : MCP *10*, M110 003699.

Vella, P., Barozzi, I., Cuomo, A., Bonaldi, T., and Pasini, D. (2011). Yin Yang 1 extends the Myc-related transcription factors network in embryonic stem cells. Nucleic acids research.